Advances in Materials
2026, Vol. 15, No. 4, pp. 161–171
https://doi.org/10.11648/j.am.20261504.13

Research Article

Theoretical Study of the Optical Performance of a Silicon Solar Cell Coated with Anti-Reflective Layers: Refractive Index, Reflectance and External Quantum Efficiency

Moulaye Diagne[1], Abel Sambou[2], Ismaila Badji[1], Oumar Absatou Niasse[1], Bassirou Ba[1, *]

[1]Semiconductor and Solar Energy Laboratory, Cheikh Anta Diop University, Dakar, Senegal

[2]Photonics and Nanofabrication Laboratory, Cheikh Anta Diop University, Dakar, Senegal

Abstract

Optical losses due to surface reflection remain one of the major factors limiting the conversion efficiency of silicon solar cells, since a significant fraction of incident light is reflected before it can be absorbed and converted into electrical energy. This paper presents a theoretical study of the optical performance of a silicon solar cell coated with anti-reflective layers, with the aim of reducing this reflection and increasing the fraction of incident light available for conversion. The refractive index of silicon was calculated using Sellmeier's equation, and the reflectance of bare silicon was derived from the Fresnel relation at normal incidence. Four coating materials — MgF_2, SiO_2, ZrO_2 and TiO_2 — were selected for their refractive indices close to the optimal value obtained from the index-matching condition between air and silicon, evaluated at reference wavelengths of 600 nm and 800 nm, with quarter-wave optical thicknesses determined accordingly. The reflectance of the coated cell was then obtained from a multiple-interference model accounting for the Fresnel coefficients at the air/coating and coating/silicon interfaces, while the external quantum efficiency was computed from a one-dimensional minority-carrier transport model over a wavelength range of 400 to 900 nm. The theoretical results showed that bare silicon has a high reflectance coefficient, ranging from 33 to 55 per cent, which justifies the deposition of an anti-reflective coating. Among the materials studied, ZrO2 and TiO2 offer the greatest reductions in reflectance, enabling the external quantum efficiency to be improved from 63 per cent for bare silicon to 95 per cent for the coated cell. These results establish the optical basis on which the electrical performance of the coated cell, examined in a companion study, can be understood. Consequently, silicon solar cells equipped with an anti-reflective coating, particularly one made of ZrO2, offer considerable potential for reducing optical losses and improving the overall performance of photovoltaic devices.

Keywords

Silicon, Anti-Reflective Coating, Refractive Index, Reflectance, External Quantum Efficiency

*Correspondence: Bassirou Ba (bassirou.ba@ucad.edu.sn)

Received: 3 September 2026; **Accepted:** 21 October 2026; **Published:** 16 November 2026

Copyright: © The Author(s), 2026. Published by Science Publishing Group. This is an **Open Access** article, distributed under the terms of the Creative Commons Attribution 4.0 License (http://creativecommons.org/licenses/by/4.0/), which permits unrestricted use, distribution and reproduction in any medium, provided the original work is properly cited.

1. Introduction

Photovoltaic energy is playing an increasingly important role amongst renewable energy sources, driven by the need to reduce dependence on fossil fuels. Indeed, the global energy system is gradually moving towards decarbonisation, and the development of solar energy as a clean and sustainable resource is attracting considerable interest in both academia and industry [1]. Among the various technologies for harnessing solar energy, photovoltaic (PV) electricity generation has become a major area of research due to its advantages in terms of environmental protection, economic viability and high efficiency [2]. In a photovoltaic electricity generation system, the PV module is the central unit for energy production [3], and the power output of each module is determined by the solar cells, which are essential components that directly convert solar energy into electricity [4]. Silicon is the standard material for the manufacture of solar cells, owing to its abundance and the maturity of the technology; silicon solar cells dominate over 90 per cent of the global market thanks to their low manufacturing costs and high stability [1-3]. Various device architectures, including multilayer silicon solar cells, have also been proposed to improve their performance [22]. However, bare silicon has one major drawback: a significant proportion of the incident radiation is lost through reflection at its surface, which limits the amount of light actually absorbed and, consequently, the cell's conversion efficiency.

This limitation was identified as early as the initial development of the silicon solar cell, the invention of which dates back to the pioneering work of Chapin et al. [24], and has since prompted numerous reviews devoted to strategies for reducing optical reflection using anti-reflective coatings [6]. In recent years, thanks to advances in the fields of materials science and device physics, the photoelectric conversion efficiency of solar cells has continued to improve [5]. To overcome the limitation caused by reflection from bare silicon, the deposition of an anti-reflective coating on the cell's surface is a widely adopted solution: by utilising optical interference phenomena, such a coating significantly reduces the reflectance and improves the absorption of radiation within the active material. These technologies for reducing surface reflection thus aim to minimise light losses due to reflection at the surface of solar cells in order to increase the absorption rate of incident light, which is a key factor in improving the photoelectric conversion efficiency of solar cells [10].

For example, L. Kholee Phimu et al. [11] systematically investigated the effects of different anti-reflective coating materials on the photon absorption rate, the external quantum efficiency and the photoelectric conversion efficiency of solar cells, confirming that a SiN_x anti-reflective coating, with a refractive index of 2.0, exhibits excellent chemical stability as well as effective reflectance-reducing properties over a wide range of wavelengths [12]. Similar approaches have led to significant improvements in the optical absorption of amorphous silicon solar cells [7], whilst modelling work has helped to provide a better understanding of the electro-optical behaviour of these devices [9]. The choice of anti-reflective material, its refractive index and its thickness directly determine the effectiveness of this reduction, hence the importance of an in-depth theoretical study of their influence on the cell's performance. Other optical management strategies, such as the integration of plasmonic nanostructures (Ag, Au, Al), pursue a similar objective of reducing reflection losses and increasing absorption, with reported gains in conversion efficiency of up to 6.58 per cent [33]. Multilayer and graded-index architectures have also been widely investigated to broaden the spectral range of low reflectance [15, 39, 43-45, 47], and, in silicon heterojunction devices, transparent conductive oxide/dielectric stacks such as ITO/SiO_x and Al_2O_3/IZO, as well as reduced-TCO designs, have been optimised for the same purpose [21, 28, 29].

This work forms part of this context; its aim is to evaluate, through a theoretical approach, the impact of different anti-reflective coatings (MgF_2, SiO_2, ZrO_2 and TiO_2) on the refractive index, reflectance coefficient and external quantum efficiency of a silicon solar cell. After characterising the optical properties of bare silicon, the study examines, in turn, the influence of the material, the refractive index and the thickness of the anti-reflective coating on these optical properties.

2. Materials and Methods

2.1. Refractive Index of Silicon

The refractive index of silicon, calculated using Sellmeier's equation, varies with wavelength as shown in Table 1:

$$n(\lambda) = \sqrt{A + \frac{B\lambda^2}{\lambda^2 - C}} \quad (1)$$

with A = 9.825, B = 3.165, C = 0.1460×10^{-12} μm^2

Table 1. *Variation in the refractive index of silicon as a function of wavelength.*

λ (nm)	399.90	427.50	459.90	495.90	539.00	590.40	652.50	729.30	826.50
n	5.570	4.961	4.583	4.320	4.123	3.969	3.847	3.752	3.673

2.2. Reflectance Coefficient of Bare Silicon

At normal incidence, the reflection coefficient R of bare silicon is given by:

$$R = \left(\frac{1-n_2}{1+n_2}\right)^2 \quad (2)$$

where n_2 is the refractive index of silicon.

2.3. Optimal Refractive Index of the Anti-Reflective Coating

The anti-reflection coating matches the refractive indices between air (n_1) and silicon (n_3) in order to create destructive interference between the waves reflected at the two interfaces, thereby minimising reflection [12]. This condition is achieved for a thickness of

$$d = \frac{\lambda}{4n_2} \quad (3)$$

which leads, for a zero reflected field, to the relation $n_2 = \sqrt{n_1 n_3}$.

For λ_{ref} = 800 nm, the optimal index is

$$n_{ARC} = \sqrt{n_{air} \cdot n_{Si}} = 1.9365 \quad (4)$$

The materials studied (MgF_2, SiO_2, ZrO_2, TiO_2) were selected for their refractive indices close to this value and their low absorption (Table 2). The choice of transparent, low-absorption materials deposited on silicon is a key criterion, as illustrated by the hole-transport layers studied for the recombination junction of perovskite/silicon cells, whose measured optical bandgaps (ranging from 1.61 to 3.57 eV depending on the material) directly determine the optical transmission to the active layer [34]. Furthermore, the thermal stability of dielectric stacks, such as that reported for Al_2O_3/SiON structures intended for the passivation of crystalline silicon cells [18], as well as the microstructural and optical characterisation of silicon-oxygen-nitrogen films produced by plasma-assisted atomic layer deposition [13], are important factors to consider for the durability of anti-reflective coatings.

Table 2. *Refractive indices of the selected materials [19, 28, 38].*

Material	MgF_2	SiO_2	ZrO_2	TiO_2
Index n	1.37	1.46	1.95	2.20

Table 3. *Optimal thicknesses for the different materials [14].*

Materials for the anti-reflective coating	MgF_2	SiO_2	ZrO_2	TiO_2
Thickness (nm) for λ = 400 nm	72	64	44	35
Thickness (nm) for λ = 800 nm	145	130	92	79

2.4. Effect of Anti-Reflective Coatings on the Reflectance of Silicon

Where an anti-reflective coating is present, the reflectance coefficient results from multiple interference between the air/coating and coating/silicon interfaces [16]:

$$r = r_{12} + \frac{t_{12}r_{23}t_{21}e^{j\varphi}}{1-r_{23}r_{21}e^{j\varphi}}, \quad \varphi = \frac{4\pi}{\lambda}n_2 e \quad (5)$$

where r_{12}, r_{21}, r_{23}, t_{12}, t_{21} are the Fresnel coefficients at the interfaces in question, and e is the thickness of the layer. These values are consistent with those reported for the influence of SiN_x: H and SiO_x films on the optical and passivation properties of anti-reflective coatings applied to silicon solar cells [46].

2.5. Photocurrent and External Quantum Efficiency

In this study, the calculations are carried out on the assumption that the transport of excess minority carriers occurs solely in the direction perpendicular to the junction, which allows the results to be expressed in one-dimensional space. This assumption is realistic insofar as the lateral dimensions of the cell are much greater than its thickness. The external quantum efficiency is thus calculated using a one-dimensional model shown in Figure 1. One-dimensional analytical and numerical models of this type are widely used to analyse the spectral response of heterojunction, thin-film and perovskite solar cells [35, 36, 40-42].

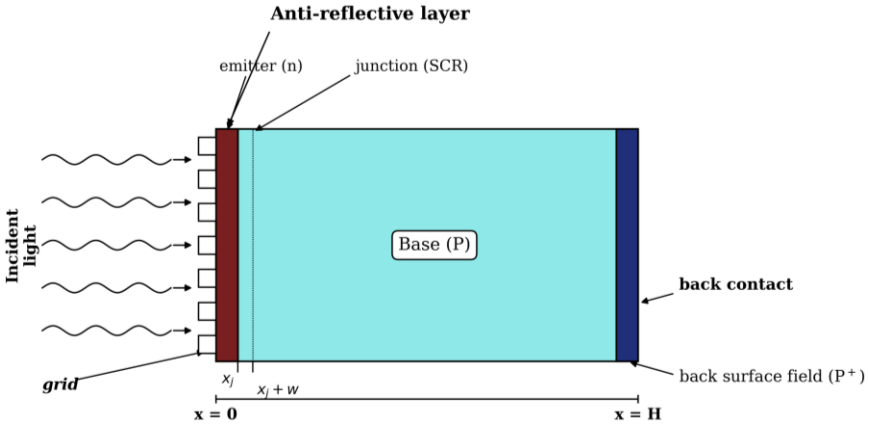


Figure 1. *One-dimensional photovoltaic cell model.*

X_j = He, W, X − X_j = Hb and X = H are, respectively, the thicknesses of the emitter, the space charge region, the base and the cell. The origin of the x-axis is taken inside the space charge region; the electric field is assumed to be practically zero in the two quasi-neutral regions; and the cell is under constant bias.

For a non-equilibrium situation, the general one-dimensional transport equation for electrons in the p-region is given by:

$$\frac{\partial(n_p-n_{p0})}{\partial t} = D_n \frac{\partial^2(n_p-n_{p0})}{\partial x^2} + \mu_n E(x) \frac{\partial(n_p-n_{p0})}{\partial x} + \mu_n (n_p - n_{p0}) \frac{\partial E(x)}{\partial x} - \frac{n_p-n_{p0}}{\tau_n} + G_n(x) \quad (6)$$

and, for the holes in zone n:

$$\frac{\partial(p_n-p_{n0})}{\partial t} = D_p \frac{\partial^2(p_n-p_{n0})}{\partial x^2} + \mu_p E(x) \frac{\partial(p_n-p_{n0})}{\partial x} + \mu_p (p_n - p_{n0}) \frac{\partial E(x)}{\partial x} - \frac{p_n-p_{n0}}{\tau_p} + G_p(x) \quad (7)$$

where (n_p − n_{p0}) and (p_n − p_{n0}) are the excess minority carrier densities in the p- and n-regions, D_n and D_p are the diffusion coefficients, μ_n and μ_p are the mobilities, E (x) is the electric field, τ_n and τ_p are the lifetimes, n_{p0} and p_{n0} are the equilibrium densities, and G_n and G_p are the generation rates of electrons and holes.

Considering the case where one of the materials is more heavily doped, these equations decouple by neglecting the term ∂E/∂x as well as the electric field in the quasi-neutral regions. In steady state, the continuity equations in the base and emitter are written respectively as:

$$D_n \frac{d^2(n_p-n_{p0})}{dx^2} + \alpha F(1-R)e^{-\alpha x} - \frac{n_p-n_{p0}}{\tau_n} = 0 \quad (8)$$

$$D_p \frac{d^2(p_n-p_{n0})}{dx^2} - \frac{p_n-p_{n0}}{\tau_n} + G(\lambda) = 0 \quad (9)$$

These two second-order differential equations have the following general solutions:

$$n_p - n_{p0} = \frac{\alpha F(\lambda)(1-R(\lambda))\tau_n}{\alpha^2 L_n^2 - 1} e^{\alpha(x_j-w)} \times A \quad (10)$$

with

$$A = \cosh\left(\frac{X-X_j-W}{L_n}\right) - e^{-\alpha(x-x_j-w)} \left\{ \frac{\frac{S_n L_n}{D_n}\left(\cosh\frac{H}{L_n} - e^{-\alpha H}\right) + \alpha L_n e^{-\alpha H}}{\frac{S_n L_n}{D_n}\sinh\frac{H}{L_n} + \cosh\frac{H}{L_n}} \right\} \sinh\left(\frac{X-X_j-W}{L_n}\right)$$

$$p_n - p_{n0} = \frac{\alpha F(1-R)\tau_n}{\alpha^2 L_p^2 - 1} \left\{ \frac{\left(\frac{S_p L_p}{D_p} + \alpha L_p\right)\sinh\frac{X_j - X}{L_p} + \left(\frac{S_p L_p}{D_p}\sinh\frac{X}{L_p} + \cosh\frac{X}{L_p}\right)e^{-\alpha x_j}}{\frac{S_p L_p}{D_p}\sinh\frac{X_j}{L_p}} - e^{-\alpha x} \right\} \quad (11)$$

The external quantum efficiency is derived from the photocurrent density using the following formula:

$$EQE = \frac{J_{ph}}{qF(\lambda)} \quad (12)$$

where J_{ph} represents the short-circuit photocurrent density. This density is given, in the emitter, the base and the space-charge region respectively, by:

$$Je_{ph} = \frac{qF(1-R)\alpha L_p}{\alpha^2 L_n^2 - 1}\left\{\frac{S_p L_p}{D_n} + \alpha L_p - \frac{\frac{S_p L_p}{D_p}\cosh\frac{X_j}{L_p} + \sinh\frac{X}{L_p}e^{-\alpha x}}{\frac{S_p L_p}{D_p}\sinh\frac{X_j}{L_p} + \cosh\frac{X_j}{L_p}} - \alpha L_p(-\alpha x)\right\} \quad (13)$$

$$Jn_{ph} = \frac{qF(1-R)\alpha L_n}{\alpha^2 L_n^2 - 1}e^{-\alpha(x_j+w)}\left\{\alpha L_n - \frac{S_n L_n}{D_n}\frac{\cosh\frac{He}{L_n} - e^{-\alpha He} + \sinh\frac{He}{L_n} + \alpha L_n e^{-\alpha He}}{\frac{S_n L_n}{D_n}\sinh\frac{He}{L_n} + \cosh\frac{He}{L_n}}\right\} \quad (14)$$

$$J_{ZCE} = qF(1-R)[1 - e^{-\alpha W}]e^{-X_j} \quad (15)$$

Thus, the total external quantum efficiency resulting from the contribution of the various regions of the cell is given by:

$$EQE = EQE_b + EQE_e + EQE_{ZCE}$$

where:

$$EQE_b = \frac{(1-R)\alpha_n L_n}{\alpha_n^2 L_n^2 - 1}e^{-\alpha_n(X_j+W)}\frac{S_n L_n}{D_n}\frac{\cosh\frac{Hb}{L_n} - e^{-\alpha Hb} + \sinh\frac{Hb}{L_n} + \alpha L_n e^{-\alpha Hb}}{\frac{S_n L_n}{D_n}\sinh\frac{Hb}{L_n} + \cosh\frac{Hb}{L_n}} \quad (16)$$

$$EQE_e = \frac{(1-R)\alpha_p L_p}{\alpha_p^2 L_p^2 - 1}\left\{\frac{\frac{S_p L_p}{D_p} + \alpha_p L_p - e^{-\alpha_p X_j}\left(\frac{S_p L_p}{D_p}\cosh\frac{X_j}{L_p} + \sinh\frac{X_j}{L_p}\right)}{\frac{S_p L_p}{D_p}\sinh\frac{X_j}{L_p} + \cosh\frac{X_j}{L_p}} - \alpha_p L_p e^{-\alpha_p X_j}\right\} \quad (17)$$

$$EQE_{ZCE} = (1-R)[1 - e^{-\alpha W}]e^{-X_j} \quad (18)$$

The total photocurrent density is the sum of the densities of the three regions (P-N-ZCE) of the photovoltaic cell [25]:

$$J_{ph} = J_n + J_p + J_{zce} \quad (19)$$

The total photocurrent J_{Total} is obtained by integrating the photocurrent density J_{ph} over the entire range of the solar spectrum used:

$$J_{Total} = \int_{\lambda_{\min}}^{\lambda_{\max}} J_{ph} \cdot d\lambda \quad (20)$$

2.6. Power and Efficiency of the Solar Cell

The power delivered by the cell is P = I ·V, and is at its maximum when $P_m = I_m \cdot V_m$ (condition dP/dV = 0). The form factor FF and the conversion efficiency η are derived from this:

$$FF = \frac{I_m V_m}{I_{cc} V_{OC}} \quad (21)$$

$$\eta = \frac{P_m}{P_{in}} \quad (22)$$

3. Results

3.1. Refractive Index of Silicon

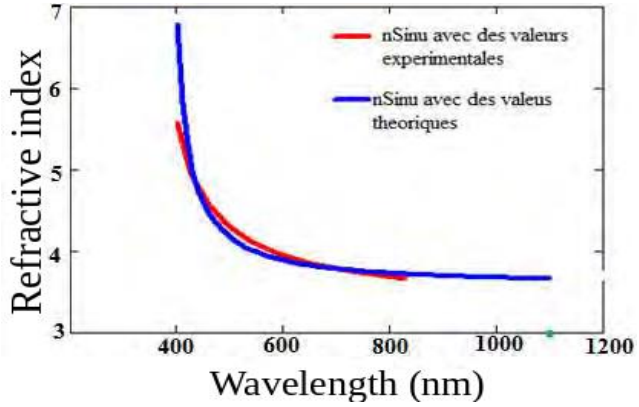


Figure 2. *Characteristics of the variation in the refractive index n of bare silicon for different experimental and theoretical values as a function of wavelength.*

This figure shows that the variations in the theoretical and experimental values of the refractive index of silicon as a function of wavelength are the same.

3.2. Reflectance of Bare Silicon

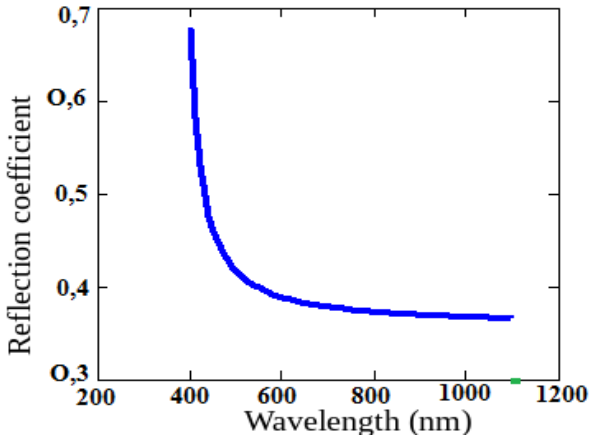


Figure 3. *Graph showing the variation in the reflection coefficient of bare silicon as a function of wavelength.*

Figure 3 shows the effect of wavelength on the reflectance of bare silicon. Over a wavelength range of 400 to 580 nm, the rate at which the reflectance coefficient decreases falls rapidly, varying from 55 per cent to 35 per cent; from 580 nm to 860 nm, this decrease slows to 33 per cent, at which point it becomes constant. A virtually identical trend has been reported for bare silicon in the literature [30, 31].

We can therefore conclude that a higher wavelength reduces the reflectance of bare silicon. Furthermore, it can be noted that the minimum reflectance lies between 33 and 36 per cent; consequently, silicon is highly reflective, which demonstrates that the use of an anti-reflective coating is necessary to reduce this reflectance.

3.3. Effect of Anti-Reflective Coatings on the Reflectance of Silicon

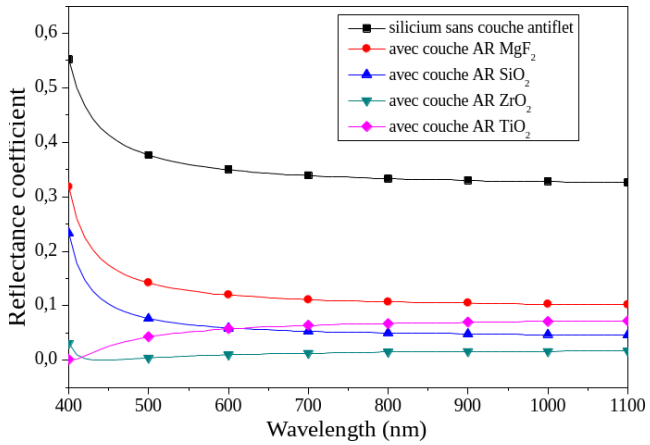


Figure 4. *Characteristics of the variation in the reflectance coefficient of bare silicon and silicon with different anti-reflective coatings as a function of wavelength: for a reference wavelength λ_{ref} = 600 nm.*

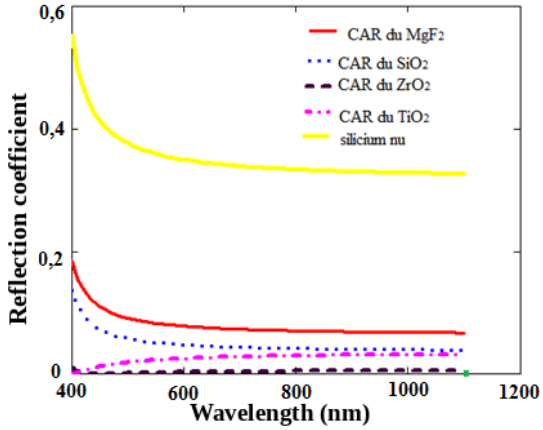


Figure 5. *Characteristics of the variation in the reflectance coefficient of bare silicon and silicon with different anti-reflective coatings as a function of wavelength: for a reference wavelength λ_{ref} = 800 nm.*

For reference wavelengths λ = 600 nm and 800 nm, the gradient in the reflectance coefficient of bare silicon and silicon coated with various anti-reflective layers of different refractive indices was investigated (Figures 4 and 5). At 600 nm (Figure 4), the reflectance of silicon coated with MgF_2 and SiO_2 increases between 400 and 560 nm, then stabilises from 870 nm onwards for SiO_2 and ZrO_2; for ZrO_2 and TiO_2, reflection is zero from 400 to 420 nm and then increases gradually, stabilising at 870 nm in the case of ZrO_2, whilst it remains virtually zero across the entire range for TiO_2 (at most 0.4% beyond 850 nm). In terms of extremes, MgF_2, SiO_2 and TiO_2 exhibit minimum and maximum reflectance values of 6.7 per cent and 18.5 per cent, 3.2 per cent and 13.6 per cent, and 0 per cent and 3.1 per cent respectively, whilst ZrO_2 remains at zero. It is also noted that an increase in the refractive index of the anti-reflective coating to a value below 1.87 proportionally reduces reflection as a function of wavelength, with the opposite effect occurring above this threshold. At 800 nm (Figure 5), the behaviour is virtually identical, with the exception that ZrO_2 exhibits zero reflection across the entire wavelength range studied.

These results show that, following the deposition of an anti-reflective coating, reflection decreases with wavelength, and that the choice of material depends on its refractive index: indices close to 2 are the most suitable, as reflection increases with wavelength beyond this value. ZrO_2 and TiO_2 are therefore the best choices for anti-reflective coatings on silicon, with zero reflectance for the former and 3.2 per cent for the latter; a reflectance of the same order of magnitude has also been reported for TiO_2 and SiO_2-based stacks [4, 26], a similar trend being confirmed for a Ta_2O_5 coating, whose refractive index, close to the optimal value, results in virtually zero reflectance (0.42 per cent at 600 nm) on silicon [37]. This near-zero reflectance achieved with a single monolayer of ZrO_2 even surpasses the 5.10 per cent reported for an optimised SiO_x/SiN_x anti-reflective double layer on conventional silicon [32].

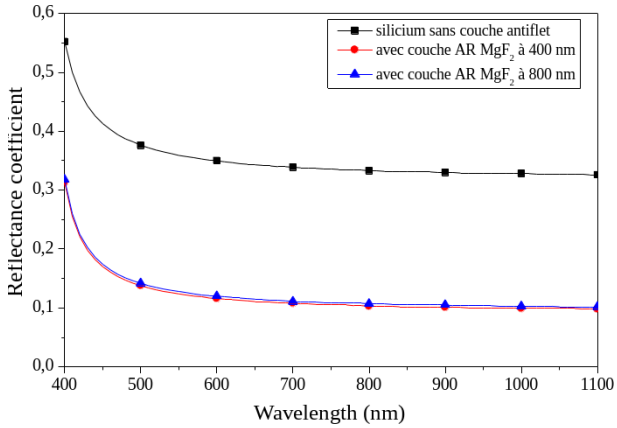


Figure 6. *Reflectance of silicon as a function of wavelength (bare silicon and silicon coated with an MgF_2 anti-reflective layer at reference wavelengths of 400 and 800 nm).*

For wavelengths centred at 400 nm and 800 nm, the variation in the reflection coefficient of silicon without an anti-reflection coating and with an MgF_2 anti-reflection coating was investigated, as shown in Figure 6. The optimum thicknesses of the anti-reflection coating to achieve destructive interference at wavelengths of 400 and 800 nm are 72 and 145 nm, respectively.

It can be seen that, for a visible wavelength range between 400 and 600 nm, the reflectance of silicon coated with MgF_2 as an anti-reflective coating for the two reference wavelengths (Figure 6) decreases gradually to reach a value below 15 per cent, at which point it remains constant up to 1100 nm. It is also noted that the two reflectance coefficients are virtually identical within the visible wavelength range. It should be noted that the optimum thicknesses of the anti-reflection coating are given in Table 3.

Furthermore, it is worth noting the benefit of the anti-reflection layer, which reduces the reflection coefficient of silicon in the long-wavelength range from 35 per cent to 10 per cent.

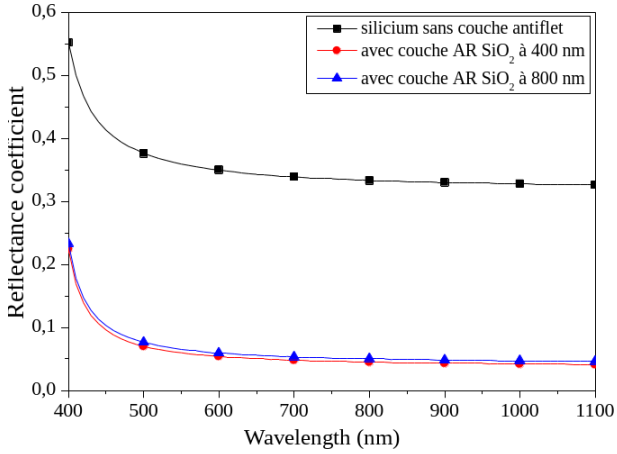


Figure 7. *Reflectance of silicon as a function of wavelength (bare silicon and silicon coated with an SiO_2 anti-reflective layer at the reference wavelengths of 400 nm and 800 nm).*

Figure 7 shows the variation in the reflectance coefficient of silicon coated with a layer of silicon dioxide (SiO_2) 64 nm and 130 nm thick, respectively, for the reference wavelengths of 400 nm and 800 nm. The same trend is observed as in the case of magnesium fluoride (MgF_2) within the same wavelength range. However, the reflection coefficients are lower at longer wavelengths (4.9 per cent for the 400 nm reference and 4.7 per cent for the 800 nm reference). When compared with MgF_2, SiO_2 is found to be more advantageous in that reflection losses are lower and the thickness of the anti-reflection coating required is smaller.

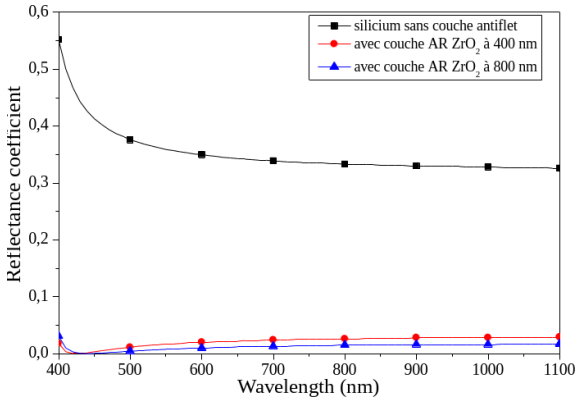


Figure 8. *Reflectance of silicon as a function of wavelength (bare silicon and silicon coated with a ZrO_2 anti-reflective layer at reference wavelengths of 400 nm and 800 nm).*

The same study was carried out in the case where the anti-reflective coating was made of zirconium oxide (ZrO_2) with layer thicknesses of 44 nm and 92 nm at 400 nm and 800 nm respectively. It is observed that the reflectance of silicon with a ZrO_2 anti-reflective coating for the two reference wavelengths decreases from 400 to 430 nm, where it becomes zero. It increases slightly and stabilises, for longer wavelengths, at 2.8 per cent and 1.7 per cent for the 400 nm and 800 nm references respectively.

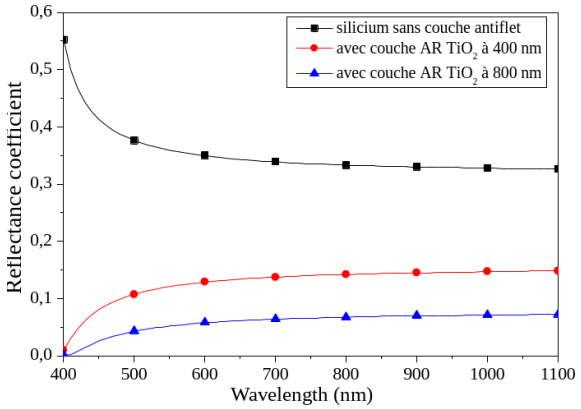


Figure 9. *Reflectance of silicon as a function of wavelength (bare silicon and silicon coated with a TiO_2 anti-reflective layer at reference wavelengths of 400 nm and 800 nm).*

The titanium oxide (TiO_2) anti-reflective coating exhibits behaviour that differs from the previous cases studied. The reflection coefficient is observed to increase from low wavelengths onwards, before becoming virtually constant at low incident photon energies. Furthermore, calculations carried out using the reference wavelengths (400 and 800 nm) yield markedly different reflectance coefficients across the entire visible spectrum. At longer wavelengths, the reflectance is 14.5 per cent for the 400 nm reference and 7 per cent for the 800 nm reference. For TiO_2, when compared with SiO_2, the advantage lies in the deposition of layers with optimal thicknesses that are 35 and 80 nm thinner for the references mentioned; however, it is less efficient at reducing reflection losses.

3.4. Spectral Response of the Silicon Solar Cell, Bare and Coated with Anti-Reflective Layers

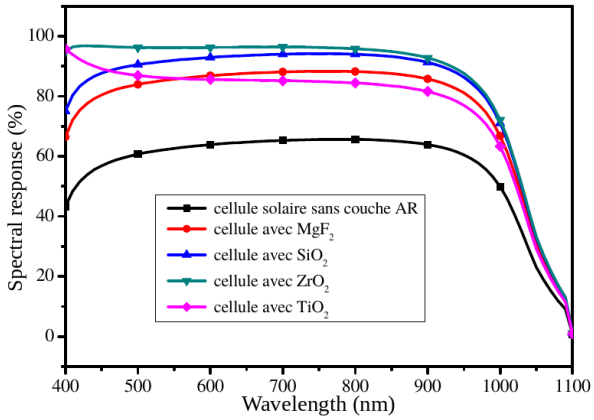


Figure 10. *Spectrum of the external quantum efficiency of bare silicon and silicon with different anti-reflective coatings as a function of wavelength.*

Figure 10 shows the variation in external quantum efficiency (EQE), or spectral response, as a function of wavelength, for a reference wavelength $\lambda = 600$ nm and by varying the refractive indices as previously described. Two regimes can be distinguished: between 400 and 850 nm, the EQE increases, rising from 28.74 per cent to 63.61 per cent for bare silicon and from 52.5 per cent to 95 per cent for silicon with an anti-reflective coating — this increase is explained, for bare silicon, by the material's heightened sensitivity in this range (as the radiation energy approaches the silicon bandgap), and, for coated silicon, by the reduction in reflection caused by the anti-reflective coating, which enhances absorption. Beyond 850 nm and up to 1100 nm, outside the visible spectrum, the EQE decreases rapidly, as the energy of the photons becomes too low to excite carriers capable of passing through the anti-reflective coating.

Furthermore, the various anti-reflective coatings (Table 2) exhibit distinct spectral responses: as with the reflectance coefficient (Figures 4 and 5), the external quantum efficiency (EQE) of the silicon cell follows the order $ZrO_2 > TiO_2 > SiO_2 > MgF_2$, confirming the decisive influence of the refractive index on the spectral response (Figure 10).

4. Discussion

The results obtained confirm that bare silicon is intrinsically a poor absorber of incident light in the absence of surface treatment, with a reflectance coefficient of between 33 and 55 per cent depending on wavelength, in agreement with earlier simulation studies [30, 31]. The deposition of a quarter-wave anti-reflective coating, whose optimal refractive index is fixed by the geometric-mean condition $n_{ARC} = \sqrt{(n_{air}\, n_{Si})}$, is shown to be a straightforward and effective route to suppressing this loss.

Among the four dielectrics investigated, the material's refractive index appears as the governing parameter: coatings with indices close to 2 (ZrO_2, TiO_2) markedly outperform lower-index materials (MgF_2, SiO_2), reducing the reflectance to near zero over most of the spectral range considered. This trend is consistent with reports for TiO_2- and SiO_2-based stacks [4, 26] and with the near-zero reflectance obtained with a Ta_2O_5 coating whose index lies close to the optimum [37]; it also compares favourably with the 5.10 per cent minimum reported for an optimised SiO_x/SiN_x double layer on conventional silicon [32]. Beyond an index of about 1.87, however, the benefit of a further increase in refractive index is reversed, which explains why TiO_2 ($n = 2.20$) is slightly less effective than ZrO_2 ($n = 1.95$) at the longest wavelengths, even though both remain far superior to MgF_2 and SiO_2.

The gain in external quantum efficiency — from 63 per cent for bare silicon to 95 per cent for the coated cell — mirrors this ranking and is of the same order of magnitude as the improvements reported for optimised single- and double-layer anti-reflective architectures on silicon and silicon-heterojunction cells [20, 27, 31, 37, 38]. Taken together, these optical results establish the basis on which the electrical output of the coated cell (short-circuit current, open-circuit voltage, fill factor and power) can be analysed, which is the object of a companion study.

5. Conclusions

This theoretical study assessed the impact of four anti-reflective coatings (MgF_2, SiO_2, ZrO_2 and TiO_2) on the optical performance of a silicon solar cell. Bare silicon has a high reflectance coefficient, ranging from 33 to 55 per cent, which fully justifies the use of an anti-reflective coating. Of the materials studied, ZrO_2 and TiO_2 offer the greatest reductions in reflectance and improve the external quantum efficiency from 63 per cent (bare silicon) to 95 per cent (coated cell). These results confirm that the deposition of an anti-reflective coating, particularly ZrO_2, is an effective and straightforward method

for significantly reducing optical losses in silicon solar cells; their impact on the cell's electrical output (current-voltage characteristic and power) is examined in a companion study.

It should be noted that this study does not take into account the effect of temperature on the optical properties of the cell [8, 23], nor surface texturing effects [17], which could complement this theoretical analysis in future work.

Abbreviations

PV	Photovoltaic
ARC	Anti-Reflective Coating
EQE	External Quantum Efficiency
FF	Fill Factor
ZCE	Space Charge Region

Author Contributions

Moulaye Diagne: Conceptualization, Data curation, Formal Analysis, Investigation, Methodology, Software, Writing – original draft

Abel Sambou: Formal Analysis, Investigation, Validation, Writing – review & editing

Ismaila Badji: Formal Analysis, Software, Visualization

Oumar Absatou Niasse: Resources, Supervision, Validation, Writing – review & editing

Bassirou Ba: Conceptualization, Project administration, Supervision, Validation, Writing – review & editing

Conflicts of Interest

The authors declare no conflicts of interest.

References

[1] Liangwei Chen, Jingwen Zhang, Xinyue Zhang, Hao Liu, « A new low-carbon project scheduling problem with renewable and traditional energy: a comprehensive analysis and its solution », *Journal of Cleaner Production*, volume 468, 2024, pp. 143089, https://doi.org/10.1016/j.jclepro.2024.143089

[2] Richard Hanna, Phil Heptonstall, Robert Gross, « Job creation in a low carbon transition to renewables and energy efficiency: a review of international evidence », *Sustainability Science*, volume 19, 2024, pp. 125–150, https://doi.org/10.1007/s11625-023-01440-y

[3] Menghan Li, Xiaoxiao Liu, Mian Yang, « Analyzing the regional inequality of renewable energy consumption and its driving factors: evidence from China », *Renewable Energy*, volume 223, 2024, pp. 120043, https://doi.org/10.1016/j.renene.2024.120043

[4] Zhixin Qian, Tao He, Haozhe Wang, Shi Peng, Jing Zhang, Xu Yu, «Recoating by atmospheric pressure plasma jet dual-layer SiO2/TiO2 films for in-situ restoration of the anti-reflective coating on solar cell modules », *Surfaces and Interfaces*, volume 74, 2025, pp. 107683, https://doi.org/10.1016/j.surfin.2025.107683

[5] Arafa H. Aly, Hassan Sayed, Hussein A. Elsayed, «Development of the monolayer silicon solar cell based on photonic crystals », *Silicon*, volume 11, 2019, pp. 1377–1382, https://doi.org/10.1007/s12633-018-9936-7

[6] Chunxue Ji, Wen Liu, Yidi Bao, Xiaoling Chen, Guiqiang Yang, Bo Wei, Fuhua Yang, Xiaodong Wang, «Recent applications of antireflection coatings in solar cells », *Photonics*, volume 9, 2022, pp. 906, https://doi.org/10.3390/photonics9120906

[7] Hussein A. Elsayed, Hassan Sayed, T. A. Taha, Abdullah G. Alharbi, Asma M. Alenad, Basheer A. Alshammari, Ashour M. Ahmed, Ahmed Mehaney, Arafa H. Aly, «Simple and efficient design towards a significant improvement of the optical absorption of amorphous silicon solar cell », *Journal of Quantitative Spectroscopy and Radiative Transfer*, volume 275, 2021, pp. 107890, https://doi.org/10.1016/j.jqsrt.2021.107890

[8] E. Radziemska, «The effect of temperature on the power drop in crystalline silicon solar cells », *Renewable Energy*, volume 28, n°1, 2003, pp. 1–12, https://doi.org/10.1016/S0960-1481(02)00015-0

[9] K. Kacha, F. Djeffal, H. Ferhati, D. Arar, M. Meguellati, «Numerical investigation of a double-junction a: SiGe thin-film solar cell including the multi-trench region », *Journal of Semiconductors*, volume 36, n°6, 2015, pp. 064004, https://doi.org/10.1088/1674-4926/36/6/064004

[10] Yuqiang Liu, Yajuan Li, Yiliang Wu, Guangtao Yang, Luana Mazzarella, Paul Procel-Moya, Adele C. Tamboli, Klaus Weber, Mathieu Boccard, Olindo Isabella, Xinbo Yang, Baoquan Sun, «High-efficiency silicon heterojunction solar cells: materials, devices and applications », *Materials Science and Engineering: R: Reports*, volume 142, 2020, pp. 100579, https://doi.org/10.1016/j.mser.2020.100579

[11] Zhaoqing Sun, Xiaoqing Chen, Yongcai He, Jingjie Li, Jianqiang Wang, Hui Yan, Yongzhe Zhang, « Toward efficiency limits of crystalline silicon solar cells: recent progress in high-efficiency silicon heterojunction solar cells », *Advanced Energy Materials*, volume 12, 2022, pp. 2200015, https://doi.org/10.1002/aenm.202200015

[12] Yunlai Yuan, Zhe Chen, Hui Peng, Xixiang Xu, Minghao Qu, Shi Yin, Xiaoning Ru, Wangping Wu, Lvzhou Li, Qinqin Wang, Jianning Ding, « Study on the process of hydrogen-doped indium oxide for silicon heterojunction solar cell mass production », *Solar Energy Materials and Solar Cells*, volume 271, 2024, pp. 112836, https://doi.org/10.1016/j.solmat.2024.112836

[13] Hong-Ping Ma, Hong-Liang Lu, Jia-He Yang, Xiao-Xi Li, Tao Wang, Wei Huang, Guang-Jie Yuan, Fadei F. Komarov, David Wei Zhang, «Measurements of microstructural, chemical, optical, and electrical properties of silicon-oxygen-nitrogen films prepared by plasma-enhanced atomic layer deposition », *Nanomaterials*, volume 8, 2018, pp. 1008, https://doi.org/10.3390/nano8121008

[14] Wei Zhang, Jielei Tu, Weixu Long, Wangfu Lai, Yuqing Sheng, Tengteng Guo, « Preparation of SiO2 anti-reflection coatings by sol-gel method », *Energy Procedia*, volume 130, 2017, pp. 72–76, https://doi.org/10.1016/j.egypro.2017.09.398

[15] Nordine Sahouane, Abdellatif Zerga, «Optimization of antireflection multilayer for industrial crystalline silicon solar cells », *Energy Procedia*, volume 44, 2014, pp. 118–125, https://doi.org/10.1016/j.egypro.2013.12.017

[16] M. Claudia Troparevsky, Adrian S. Sabau, Andrew R. Lupini, Zhenyu Zhang, «Transfer-matrix formalism for the calculation of optical response in multilayer systems: from coherent to incoherent interference », *Optics Express*, volume 18, n °24, 2010, pp. 24715–24721, https://doi.org/10.1364/OE.18.024715

[17] KartikaChandra Sahoo, Men-Ku Lin, Edward-Yi Chang, Yi-Yao Lu, Chun-Chi Chen, Jin-Hua Huang, Chun-Wei Chang, « Fabrication of antireflective sub-wavelength structures on silicon nitride using nano cluster mask for solar cell application », *Nanoscale Research Letters*, volume 4, n °7, 2009, pp. 680–683, https://doi.org/10.1007/s11671-009-9297-7

[18] Kuk-Hyun Cho, Hyo Sik Chang, « A study on the thermal stability of an Al_2O_3/SiON stack structure for c-Si solar cell passivation application », *Journal of the Korean Ceramic Society*, volume 51, n °3, 2014, pp. 197–200, https://doi.org/10.4191/kcers.2014.51.3.197

[19] A. Soutar, B. Fokkink, Z. Xianting, T. S. Nee, L. Wu, «Sol-gel Antireflective Coatings », *SIM Tech Technical Report*, 2001.

[20] Alexandros Cruz, Darja Erfurt, Philipp Wagner, Anna B. Morales-Vilches, Florian Ruske, Rutger Schlatmann, Bernd Stannowski, «Optoelectrical analysis of TCO+silicon oxide double layers at the front and rear side of silicon heterojunction solar cells », *Solar Energy Materials and Solar Cells*, volume 236, 2022, pp. 111493, https://doi.org/10.1016/j.solmat.2021.111493

[21] Can Han, Rudi Santbergen, Max van Duffelen, Paul Procel, Yifeng Zhao, Guangtao Yang, Xiaodan Zhang, Miro Zeman, Luana Mazzarella, Olindo Isabella, « Towards bifacial silicon heterojunction solar cells with reduced TCO use », *Progress in Photovoltaics: Research and Applications*, volume 30, n °7, 2022, pp. 750–762, https://doi.org/10.1002/pip.3550

[22] Martin A. Green, Alistair B. Sproul, Tom Puzzer, Guang Fu Zheng, Paul Basore, Trevor Young, « Silicon Parallel Multilayer Thin Film Solar Cells », *MRS Online Proceedings Library*, volume 426, 1996, pp. 103–110, https://doi.org/10.1557/PROC-426-103

[23] Modou Pilor, Alassane Diaw, Bouchaib Hartiti, Papa Touty Traore, Bassirou Ba, « Passive Cooling of Photovoltaic Modules Using Nanofluid Layers: Thermal Modeling and Efficiency Improvement Under Outdoor Conditions », *European Journal of Advances in Engineering and Technology*, volume 12, n °7, 2025, pp. 60–65.

[24] D. M. Chapin, C. S. Fuller, G. L. Pearson, «A New Silicon p-n Junction Photocell for Converting Solar Radiation into Electrical Power », *Journal of Applied Physics*, volume 25, 1954, pp. 676–677, https://doi.org/10.1063/1.1721711

[25] L. Remache, A. Mahdjoub, E. Fourmond, J. Dupuis, M. Lemiti, « Design of porous silicon, PECVD SiOx antireflection coatings for silicon solar cells », in Proceedings of the International Conference on Renewable Energies and Power Quality (ICREPQ), Granada, Spain, 2010, https://doi.org/10.24084/repqj08.280

[26] Abdulkarem H. M. Almawgani, Ahmad Alzahrani, Ali Hajjiah, Ahmed Mehaney, Hussein A. Elsayed, Hassan Sayed, «Optical absorption performance of CZTS/ZnO thin film solar cells comprising anti-reflecting coating of texturing configuration », *RSC Advances*, volume 13, 2023, pp. 31554–31568, https://doi.org/10.1039/d3ra05056d

[27] Bing Hao, Yimeng Song, Conghui Jiang, Jiufang Han, Yang Jiang, Zhi Deng, Wenxin Wang, Haiqiang Jia, Hong Chen, Chunhua Du, « Comparing single-, double- and triple-layer anti-reflection coatings for ultra-low reflectance in silicon heterojunction solar cells », *Japanese Journal of Applied Physics*, volume 62, 2023, pp. 061002, https://doi.org/10.35848/1347-4065/acd7b7

[28] Seok Jin Jang, Muhammad Quddamah Khokhar, Hasnain Yousuf, Alamgeer, Junhan Bae, Yeojin Jeong, Yunhui Jang, Youngkuk Kim, Sangheon Park, Woo Kyoung Kim, Junsin Yi, « Improvement of optoelectrical properties of silicon heterojunction solar cells by using ITO/SiOx DLARC with NH3 plasma treatment », *Current Applied Physics*, volume 80, 2025, pp. 72–81, https://doi.org/10.1016/j.cap.2025.09.001

[29] Muhammad Aleem Zahid, Muhammad Quddamah Khokhar, Somin Park, Shahzada Qamar Hussain, Youngkuk Kim, Junsin Yi, « Influence of Al_2O_3/IZO double-layer antireflective coating on the front side of rear emitter silicon heterojunction solar cell », *Vacuum*, volume 200, 2022, pp. 110967, https://doi.org/10.1016/j.vacuum.2022.110967

[30] N. Mbengue, M. Diagne, F. Dia, S. Ndiaye, O. A. Niasse, A. Dieye, M. Niane, B. Ba, «Simulation Study of Optical Reflection and Transmission Properties of the Anti-Reflection Coatings on the Silicon Solar Cells », *International Journal of Scientific Engineering and Technology*, volume 5, n °3, 2016, pp. 161–164, https://doi.org/10.17950/ijset/v5s3/308

[31] N. Mbengue, M. Diagne, F. Dia, M. Niane, A. Dieye, W. Diallo, O. A. Niasse, B. Ba, « Influence of the Refractive Index of Anti-Reflective Coating on the External Quantum Efficiency of the Silicon Solar Cells », *International Journal of Engineering Research*, volume 5, n °4, 2016, pp. 226–230, https://doi.org/10.17950/ijer/v5s4/401

[32] N. Mbengue, M. Diagne, M. Niane, A. Dieye, O. A. Niasse, B. Ba, « Optimization of Double Anti-Reflective Coating SiOx/SiNx on the Solar Cells with Silicon Conventional », *International Journal of Engineering Trends and Technology*, volume 20, n °2, 2015, pp. 101–104, https://doi.org/10.14445/22315381/IJETT-V20P218

[33] Akbari et al., « Designing novel plasmonic architectures for highly efficient CIGS solar cells », *Solar Energy*, volume 274, 2024, pp. 112589, https://doi.org/10.1016/j.solener.2024.112589

[34] Vasquez et al., «Optical, electrical and chemical characterization of inorganic hole transporting materials for the recombination junction in two-terminal perovskite/silicon heterojunction solar cells », *Solar Energy*, volume 273, 2024, pp. 112375, https://doi.org/10.1016/j.solener.2024.112375

[35] Pruthaba Jadeja et al., « Investigating the impact of various electron transport layers on the performance of Sn-based perovskite solar cells: A device simulation using SCAPS-1D », *Journal of Physics and Chemistry of Solids*, volume 208, 2026, pp. 113088, https://doi.org/10.1016/j.jpcs.2025.113088

[36] Ajay Kumar et al., « Advanced perspectives on chalcogenide perovskite solar cells using CZTS as HTL for optimum efficiency », *Journal of Physics and Chemistry of Solids*, volume 208, 2026, pp. 113101, https://doi.org/10.1016/j.jpcs.2025.113101

[37] M. Pilor, A. Diaw, P. T. Traore, N. Mbengue, M. Diagne, O. A. Niasse, B. Ba, «Influence of the Refraction Index, The Thickness of the Antireflection Layer, The Spectral Response and The Texturization of a Silicon Solar Cell: Application to Antireflective Multilayers », *European Journal of Advances in Engineering and Technology*, volume 10, n°5, 2023, pp. 66–75, https://doi.org/10.5281/zenodo.10636781

[38] A. Diaw, M. Pilor, N. Mbengue, P. T. Traore, « Impact of Thickness, Refractive Index and Diffusion Length of Minority Carriers on Antireflection Materials: Study on the Spectral Response of a Monocrystalline Silicon Solar Cell », *Journal of Scientific and Engineering Research*, volume 10, n°5, 2023, pp. 229–235, https://doi.org/10.5281/zenodo.10458658

[39] Z. Fang, Q. Chen, J. Yuan, «Bi-layered closed-pore structure anti-reflective coatings with ZnO quantum dots for further improving the solar cell efficiency », *Solar Energy Materials and Solar Cells*, volume 294, 2026, pp. 113936, https://doi.org/10.1016/j.solmat.2025.113936

[40] N. Mbengue, M. Diagne, M. Niane, O. A. Niasse, B. Ba, «External Quantum Efficiency of a Solar Cell ZnO/CdTe: Effect of Emitter and Base Thicknesses », *International Journal of Engineering Trends and Technology*, volume 20, n°2, 2015, pp. 105–108, https://doi.org/10.14445/22315381/IJETT-V20P219

[41] M. Diagne, W. Diallo, N. Mbengue, F. Dia, O. A. Niasse, « External Quantum Efficiency of a ZnO/CdTe Solar Cell: Effects of Space Charge Zones, Diffusion Length & Recombination Rate, Calculated by the Dielectric Function Method », *International Journal for Scientific Research & Development*, volume 6, n°7, 2018, pp. 591–594, https://www.ijsrd.com/articles/IJSRDV6I70317.pdf

[42] M. Diagne, W. Diallo, N. Mbengue, F. Dia, O. A. Niasse, B. Ba, «External Quantum Efficiency of a Solar Cell ZnO/CdTe: Effects of Excitons by the Method of Calculating the Dielectric Function », *International Journal of Engineering Sciences & Research Technology*, volume 7, n°9, 2018, pp. 300–308, https://doi.org/10.5281/zenodo.1435552

[43] A. Diaw, O. A. Niasse, N. Mbengue, B. Ba, «Simulations of Antireflecting Coating on a Monocrystalline Silicon Solar Cell: Influence of Optical Parameters on a Double Layers », *American Journal of Energy Research*, volume 11, n°1, 2023, pp. 27–30, https://doi.org/10.12691/ajer-11-1-3

[44] A. Dieye, N. Mbengue, O. A. Niasse, F. Dia, M. Diagne, B. Ba, «Influence of Multi Anti-Reflective Layers on the Silicon Solar Cells », *Journal of Materials Science & Surface Engineering*, volume 5, n°8, 2017, pp. 729–732, https://www.jmsse.in/files/584_Awa_Dieye_et_al.PDF

[45] M. M. Diop, A. Diaw, N. Mbengue, O. Ba, M. Diagne, O. A. Niasse, B. Ba, J. Sarr, «Optimization and Modeling of Antireflective Layers for Silicon Solar Cells: In Search of Optimal Materials », *Materials Sciences and Applications*, volume 9, 2018, pp. 705–722, https://doi.org/10.4236/msa.2018.98051

[46] L. Remache, E. Fourmond, A. Mahdjoub, J. Dupuis, M. Lemiti, «Influence of PECVD SiOx and SiNx:H films on optical and passivation properties of antireflective porous silicon coatings for silicon solar cells », *physica status solidi (c)*, volume 8, n°6, 2011, pp. 1893–1897, https://doi.org/10.1002/pssc.201000110

[47] A. Mahdjoub, L. Zighed, «New designs for graded refractive index antireflection coatings », *Thin Solid Films*, volume 478, 2005, pp. 299–304, https://doi.org/10.1016/j.tsf.2004.11.119

Research Field

Moulaye Diagne: Modelling of photovoltaic cells, Anti-reflective coatings, Thin-film semiconductors, Solar energy applications

Abel Sambou: Photonics, Nanofabrication, Thin films, Optical materials

Ismaila Badji: Semiconductor physics, Simulation of solar cells

Oumar Absatou Niasse: Semiconductor physics, Photovoltaics, Solar energy

Bassirou Ba: Semiconductor physics, Photovoltaic conversion, Solar energy